ST7840

Effects of End Distance and Temperature on Thin-Sheet Steel Double Shear-Bolted Connections

Yancheng Cai, M.ASCE[1] and Ben Young, F.ASCE[2]

ABSTRACT

An experimental investigation was conducted with thin sheet steel (TSS) double shear bolted connections at elevated temperatures. The connection specimens were fabricated by TSS 0.42 mm G550 and 1.90 mm G450. The specimens were designed with the variation of end distance. The tests were conducted at 5 different nominal temperature levels up to 900 °C using the steady state test method. The variation of the end distance and temperature on the behavior of the connection specimens was investigated. The increment of the connection ultimate load was found as the end distance increased up to five times the diameter of bolt. It was also found that the deteriorations of the connection strengths occurred in a similar manner to the corresponding material properties at elevated temperatures. At each nominal temperature level, as the end distance increased, the failure modes of specimens changed from tearout to bearing. The experimental results were compared with the predictions by using the international design codes for cold-formed steel structures, including NAS (2016), EC3-1.3 (2006) and AS/NZS (2018). In calculating the nominal strengths of the connections, the reduced material properties of TSS obtained at elevated temperatures were used. Overall, the predictions from the NAS, EC3-1.3 and AS/NZS were found to be conservative, with the AS/NZS providing the least conservative and least scattered predictions. In general, the NAS and AS/NZS could accurately

[1] Post-doc fellow, Dept. of Civil Engineering, The Univ. of Hong Kong, Pokfulam Rd., Hong Kong (corresponding author). E-mail: yccai@hku.hk
[2] Professor, Department of Civil and Environmental Engineering, The Hong Kong Polytechnic University, Hong Kong. E-mail: ben.young@polyu.edu.hk

predict the failure modes for TSS connection specimens that failed in tearout and bearing failure at different temperature levels.

Keywords: Bolted connection; end distance; experimental investigation; failure mode; high temperatures.

INTRODUCTION

Steel sheets are commonly used to fabricate cold-formed steel members by cold-rolling and brake-pressing methods. The structural behavior of cold-formed steel members has been investigated extensively, including beams (Laím et al. 2013; Wang and Young 2014), columns (Young and Rasmussen 1998; Young and Hancock 2003), beam-columns (Torabian et al. 2015; Torabian et al. 2016) and built-up sections (Wang and Young 2016a; Wang and Young 2016b). Bolted connections are popular in the design and construction of cold-formed steel structures. For examples, in the connections of beam-to-beam and beam-to-column, the bearing of bolt holes and shear in the bolts are commonly critical in the transfer of loadings. Investigation of single shear (single overlap) bolted connections of thin sheet steels (TSS) subjected to longitudinal tensile loading were conducted by Rogers and Hancock (1998; 1999). They proposed design rules covering the different failure modes of the connection plates, including tearout, bearing and net section tension. Some recent investigations have focused on bolted connections of cold-reduced steel sheets failed in block shear capacity (Teh and Clements 2012) and subjected to different loading directions (Teh and Uz 2014). It should be noted that these tests were conducted at ambient (room) temperature condition only, but not at high temperatures

The safety of steel structures under fire conditions is a matter of serious concern in design due to the strength and stiffness deterioration at elevated temperatures. Behavior of cold-formed

steels at elevated temperatures has been investigated, including mechanical properties (Kankanamge and Mahendran 2011, Imran et al 2018), beams (Craveiro, et. al. 2014; Laím, et. al. 2016) and columns (Laím, et. al. 2015; Craveiro, et. al. 2016). Connections and joints are one of the most critical components of structural stability for steel structures, e.g., bolted connections. The structural behavior of TSS bolted connections at elevated temperatures was investigated experimentally and numerically by Yan and Young (2011; 2012; 2013). Based on their findings, design rules were proposed for TSS double shear bolted connections at elevated temperatures that failed in the bearing of the sheets (Yan and Young 2012). End distance (e_1), i.e., the distance measured in the line of force from the center of bolt hole to the nearest edge of an adjacent hole or to the end of the plate (AS/NZS 2018), has effects on the structural behavior of a bolted connection in terms of ultimate strength and failure mode. However, it should be noted that to date there have not been any investigation into the effects of e_1 and elevated temperatures on TSS double shear bolted connections. Furthermore, the bolted connection design rules in current design specifications (NAS 2016; EC3-1.3 2006; AS/NZS 2018) are only applicable for ambient temperature condition, but not for elevated temperatures. Hence, the purpose of this study aims to investigate the effects of end distance and temperature of TSS double shear bolted connections.

In this paper, experimental investigation on the effects of e_1 on double shear bolted connections of TSS at elevated temperatures was conducted using the steady state test method. The connection specimens were fabricated by TSS 0.42 mm G550 and 1.90 mm G450. The specimens were designed with the variation of end distance, and categorized into 2 series by the ratios of diameter of bolt to thickness of connection plate. The tests were conducted at 5 different nominal temperature (T) levels, namely, at 22 °C (ambient temperature), 300 °C, 450 °C, 600 °C and 900 °C. The load-deflection curves of the specimens at different temperature levels were obtained. The variation of e_1 and T on the structural behavior of the

bolted connections was obtained, in terms of ultimate loads and failure modes. Furthermore, the experimental ultimate loads and failure modes were used to assess the applicability of the current design rules for TSS double shear bolted connections at elevated temperatures specified in the NAS (2016), EC3-1.3 (2006) and AS/NZS (2018).

STEADY STATE TEST METHOD

Tests of structural fire resistance are mainly carried out by two methods, i.e., the steady state test method and the transient state test method. In the former method, the specimen is heated to a predetermined temperature level, and then loaded until it fails; while in the latter, the specimen is loaded to a certain level, and then heated until it fails. The first method could be easier and safer in fire testing due to the displacement control mode used instead of the load control mode in operating the testing machine. It should be noted that previous research showed that the bolted connection strengths decreased in a similar manner at elevated temperatures by using the steady state test method and the transient state test method for thin sheet steel (Yan and Young 2013) and cold-formed stainless steel (Cai and Young 2015) connection specimens. In this study, the steady state test method was adopted for the tests of the coupon and connection specimens.

First, the temperature of the specimen was raised by an MTS model 653.04 high temperature furnace to a pre-determined level (i.e., 300 °C, 450 °C, 600 °C and 900 °C). The furnace is able to reach a maximum temperature of 1400 °C. The MTS high temperature furnace model 653.04 has an accuracy of ±1 °C. During the heating process, the top end of the specimen was gripped, while the bottom end was free to expand. The heating rate of the furnace was adjusted within 40-60 °C/min depending on the target temperature level, i.e., the heating rate of 40 °C/min was

used for the lower temperature level of 300 °C, while the rate of 60 °C/min was used for the higher temperature level of 900 °C. This aimed to avoid the unexpected overshoot when reaching the target nominal temperature levels, while saving the heating time. Similar heating rates were adopted for carbon steel bolted connections (Yan and Young 2011; 2013), and stainless steel bolted connections (Cai and Young 2015) tested at elevated temperatures by using steady state test method. After reaching the pre-selected temperature level, the specimen temperature was stabilized for a period of 8 to 15 minutes. This allowed the heat transfer in the specimen and ensured that the specimen temperature was in a stable state. This was monitored by the readings from the external thermocouple (RS PRO Type K thermocouple) that in contact with the surface of the specimen, i.e., in the middle of the gauge length of the coupon specimen and in the vicinity of the bolt of the connection specimen. After that, the bottom end of the specimen was gripped. A tensile load was applied to the specimen by driving the hydraulic actuator of the machine in displacement control mode. The test was conducted until the failure of the specimen, while the temperature level was maintained throughout. A data acquisition system was used to record the temperatures, strains, deflections (elongations) and applied loads of the specimen at regular intervals during the test.

COUPON TESTS

The TSS 0.42 mm G550 and 1.90 mm G450 were used in this study, The TSS grade G550 had a nominal thickness (t) of 0.42 mm, while that of the grade G450 was t = 1.90 mm. The material properties of the TSS at elevated temperatures were measured by coupon tests in an MTS testing machine. The TSS coupon specimens were cut in the rolling direction, and had the same

dimensions as those tested by Yan and Young (2011). The tests were conducted at 5 different nominal temperature levels, namely, at 22 °C, 300 °C, 450 °C, 600 °C and 900 °C. The temperature levels were selected based on the reduction trends in TSS material properties and TSS connection strengths at elevated temperatures conducted by Yan and Young (2013). The internal thermocouples of the furnace were not in contact with the test specimen, hence, an external thermocouple was used and it contacted on the surface of the test specimen in the vicinity of the bolt as mentioned earlier. The external thermocouple (RS PRO Type K) with length of 150 mm, and diameter of 0.5 mm is able to measure the temperature up to 1100 °C with an accuracy of 0.5 to 5 °C. An MTS model 632.54 F-11 high temperature axial extensometer was used to measure the strains at the gauge length of the coupon specimen. The TSS material properties at ambient temperature condition were reported by Cai and Young (2019), as shown in Table 1; while the material properties at high temperatures in this study are summarized in Table 2, including the specimen temperature (T_m), Young's modulus (E_h), longitudinal 0.2% proof stress ($f_{0.2,h}$), longitudinal ultimate strength ($f_{u,h}$), ultimate strain ($\varepsilon_{u,h}$) and fracture strain ($\varepsilon_{f,h}$).

BOLTED CONNECTION TESTS

General

In total, 43 specimens of TSS double shear bolted connections were experimentally investigated. The specimen was bolted by one high strength steel bolt with washers at both sides. The specimens were designed by varying the value of e_1 (See Fig. 1). Tensile loading was applied at the specimen two ends. The specimen ends were gripped with pin-end boundary

conditions. The applied loads, deflections (elongations), temperatures (T_m), failure modes and ultimate loads (P_u) of the bolted connection specimens were obtained.

Specimen design and labeling

The TSS connection specimens in double shear were bolted with same plate thickness, i.e., 0.42 mm or 1.90 mm. The TSS plates for the bolted connection specimens were cut from the same batch of steel sheets as those for the coupon specimens. The width (w) of the connection plates was kept as 50 mm. The length (L) of the connection plates was varied from 353 to 393 mm such that the assembled specimen length was maintained at 690 mm, where the clear distance between the grips was maintained as 560 mm. The Grade 12.9 high strength steel bolt with a nominal diameter of 8 mm (M8) was used. The nominal size of the bolt hole (d_o) was determined by following the NAS (2016) and AS/NZS (2018) specifications, where $d_o = (d + 1)$ for $d < 12$ mm. Hence, $d_o = 9$ mm was used in this study. Correspondingly, the nuts and washers were used. The specimens have washers at two sides. The measured values of the bolt diameter and dimensions of the washer are detailed in Cai and Young (2019). The diameters of the bolts were designed such that the assembled connection specimens were mainly failed in plate bearing but not in bolt shear based on the design calculations at ambient temperature condition. It should be noted that the minimum requirement of e_1 for bolted connection specimen is $e_1 \geqslant 1.5d$ in AS/NZS (2018) and NAS (2016); or $e_1 \geqslant 1.5d_o$ in EC3-1.3 (2006). The definitions of symbols and values for the TSS plate in this study are shown in Fig. 1.

The TSS bolted connection specimens were divided into two groups by the nominal values of d/t, namely, $d/t = 19.05$ for 0.42 mm G550 and $d/t = 4.21$ for 1.90 mm G450. In each group, four specimen series were designed by the variation of e_1, where $e_1 = 1.0d$, $3d$, $5d$ and $6d$. Each specimen series was tested at 5 different nominal temperature levels as those for the coupon tests, namely, at 22 °C, 300 °C, 450 °C, 600 °C and 900 °C. Hence, the effects of e_1 and T on

the behavior of bolted connections could be obtained. Generally, for a given e_1 in each TSS grade, five specimens were tested. The design of the TSS double shear bolted connection specimens are summarized in Table 3. Totally, 43 TSS double shear bolted connection specimens were designed and tested, where 21 specimens were designed for TSS 0.42 mm G550, including one repeated test; and 22 specimens were designed for TSS 1.90 mm G450, including 2 repeated tests, as detailed in the specimen labeling in Tables 4-8. The specimens were generally labelled by three segments such that the connection plate thickness (t), connection type and e_1 could be identified. For example in the specimen labelling shown in Table 4, the first segment of "042" and "190" stand for the TSS of 042 mm G550 and 1.90 mm G450, respectively; "D" is short for double shear bolted connection; and the third segment shows the value of e_1. The letter "r" in the last indicates that it is a repeated test. Hence, the bolted connection specimens could be identified in series, either by T or by e_1, for example, Series 042-D-d at elevated temperatures or Series 042-D at 300 °C.

Testing procedure

Tests of the TSS double shear bolted connections were conducted in the same MTS machine as for the coupon tests. At ambient temperature condition, two Linear Voltage Differential Transducers (LVDTs) were used to measure the deflections (elongations) that covered a distance of 200 mm in the middle part of the specimen. At high temperature conditions, the LVDTs were removed; instead, the aforementioned high temperature furnace was used to raise the temperature of the specimen. Similar to the coupon tests, the RS PRO Type K thermocouple was used to measure the temperature of the connection specimen. The specimen was assembled into a gripping apparatus that could provide pin-end boundary conditions at each end (Yan and Young 2013; Cai and Young 2014). Clips linked with iron wire were used to prevent the curling up at the connection part (Rogers and Hancock 1998, Yan and Young 2013). As mentioned

previously, the steady state test method was used for the bolted connection tests at elevated temperatures in the present study. The specimen was subjected to tensile loading with a constant rate of 1.0 mm/min. The same loading rate for bolted connections of TSS with the similar clear distance between the grips was adopted by Rogers and Hancock (1998), and Yan and Young (2013). A typical test setup for double shear bolted connection of TSS at ambient temperature and high temperature conditions is illustrated in Fig. 2.

Testing results

The behaviors of the TSS connection specimens in double shear were obtained, including the applied loads, deflections, specimen temperatures (T_m), failure modes and ultimate loads (P_u). Figs. 3-4 illustrate the respective curves of load-deflection for specimen series 042-D-3d and 190-D-3d at elevated temperatures. The horizontal axis plots the deflection of the specimens, while the vertical axis shows the corresponding applied load during the tests. The ultimate loads of the specimens at ambient temperature ($P_{u,r}$) and high temperature ($P_{u,h}$) conditions are shown in Tables 4-8. The load-deflection curves of the specimens fabricated by TSS 0.42 mm G550 showed multiple peaks and valleys at lower temperature levels (e.g, 300 °C). These were also found in the load-deflection curves in Yan and Young (2013). The drops in the curves could be due to the shear fracture of the plates. The shear fracture occurred when the bolt intruded as load increased, because of the small thickness of the plates and the brittle of the material properties. Repeated tests were conducted for the TSS double shear bolted connections at elevated temperatures, where the maximum difference of the ultimate loads between the first and second tests was 7.7%, i.e., the ultimate load of 5.32 kN for Specimen 042-D-d compared with that of 4.94 kN for Specimen 042-D-d-r at the nominal temperature of 300 °C. The measured T_m and the test failure modes are also reported in the tables. The failure modes in this study included tearout failure (T), bearing failure (B), material failure and bolt shear (BS). The

failure modes of the TSS bolted connection specimens have been characterized by Rogers and Hancock (1998), and by Yan and Young (2013).

DESIGN RULES

The current cold-formed steel codes (NAS 2016; EC3-1.3 2006; AS/NZS 2018) provide design rules for bolted connections subjected to tensile loading. Hence, in this study, these design rules were used to calculate the nominal strengths (unfactored design strengths) of the specimens. It should be noted that these design rules are applicable to ambient temperature condition only, but not for elevated temperatures. For the purpose of direct comparison and assessment, the material properties at ambient temperature were replaced by those at high temperatures in the calculations.

Different design equations associated with different failure modes for TSS bolted connections are specified in the codes (NAS 2016; EC3-1.3 2006; AS/NZS 2018). In the calculations, the predicted strength of a bolted connection specimen with the corresponding failure mode was determined by the calculated minimum nominal strength. It should be noted that a bolted connection specimen under tensile loading may fail in the connection plate by shear rupture (tearout), bearing or tension rupture (net section tension), or fail in the bolt by shear failure. The calculations of the bolted connection specimens failed due to tearout, bearing and net section tension are provided in Clauses 5.3.2-5.3.4 in the AS/NZS (2018). It should be noted that the rules apply for connection plate thicknesses between 0.42 mm and 4.76 mm (AS/NZS 2018). In addition, the net section tension strength is also governed by Clause 3.2.2 of the AS/NZS (2018). For the NAS (2016), Section J3.3 specifies the designs for the plate bearing failure, Section J6.1 for the shear rupture and Section J6.2 for the tension rupture. It should be

noted that the NAS (2016) considers the net end distance (e_{net}) instead of e_1 in the shear rupture calculation. For the EC3-1.3 (2006), the calculations for bolted connections loaded in shear are provided in Table 8.4 of Section 8.3. Note that the strength corresponding to tearout failure is incorporated into the design of the bearing failure by the coefficient of α_b, where the effect of $e_1/(3d)$ is considered. Therefore, tearout failure (shear rupture) is not specified in the EC3-1.3 (2006). In addition, the TSS 0.42 mm is beyond the limit of no less than 0.61 mm specified in the NAS (2016) for the design of the bearing strength and also outside the lowest bound, namely, the 0.75 mm, in the range of validity in the EC3-1.3 (2006). However, for a direct comparison, the design equations are applied to the TSS 0.42 mm in this study. The differences between these design rules in different specifications (NAS 2016; EC3-1.3 2006; AS/NZS 2018) are discussed in Cai and Young (2019).

EFFECTS OF END DISTANCE

Ultimate loads

The ultimate loads of the TSS double shear bolted connections affected by the variation of e_1 at different nominal temperature levels were investigated. Figs. 5-6 plot the ultimate loads against the variations of e_1 for the specimen series 042-D and 190-D, respectively. The vertical axes of the graphs show the ultimate load of each test, where the $P_{u,r}$ and $P_{u,h}$ mean the ultimate loads at ambient and high temperatures, respectively. The horizontal axes plot the ratio of e_1/d such that a direction comparison could be achieved. For both specimen series 042-D and 190-D, it is shown that the $P_{u,r}$ and $P_{u,h}$ increase obviously with the increment of e_1/d from 1 to 5 at different nominal temperature levels. At each temperature level, the increments of $P_{u,r}$ and $P_{u,h}$

are larger from e_1/d = 1 to e_1/d = 3 than those from e_1/d = 3 to e_1/d = 5. Generally, the $P_{u,r}$ and $P_{u,h}$ are maintained as the end distance increased further (i.e., from e_1/d = 5 to e_1/d = 6), which may indicate that for double shear bolted connections of TSS, the $P_{u,r}$ and $P_{u,h}$ are generally maintained when the $e_1 \geq 5d$ in this study.

Failure modes

The failure modes of the specimens obtained from the tests at different nominal temperatures are shown in Tables 4-8. Each table includes the specimen series tested at the same temperature level. For specimen series 042-D and 190-D tested at ambient temperature condition (as shown in Table 4), the specimens all failed in tearout (T) with the end distances of $e_1 = d$ and $e_1 = 3d$. At e_1/d = 1, the tearout failure mode was obvious in the specimens; while e_1/d was increased to 3, less obvious of such failure mode was found, instead, the occurrence of material splitting at the plate ends occurred (See Fig. 7(b) and Fig. 8(b)). As the end distances were increased to $e_1 = 5d$ and $e_1 = 6d$; the failure modes of tearout or material splitting at the plate ends disappeared, instead, only the plate failure mode of bearing was observed.

For specimens fabricated by TSS 042 mm at the same high temperature levels, i.e. Series 042-D, the above failure modes were similarly observed at T = 300 °C and T = 450 °C. However, the failure mode of material failure (MF), failed beyond the overlapped connection part as found by Yan and Young (2013), took over at 600 °C and 900 °C when $e_1 = 5d$ and $e_1 = 6d$ (see Tables 7 and 8, and Fig. 10(c)-(d)). For the specimen Series 190-D, the aforementioned failure modes at ambient temperature were also similarly observed at the nominal high temperatures of 300 °C, 450 °C and 600 °C. However, the specimens failed in bolt shear (BS) at 900 °C when the $e_1 = 5d$ and $e_1 = 6d$ (see Table 8). The specimens changed the failure modes from bearing failure to other failure modes at higher temperature levels, this may be due to the larger bearing resistances achieved at higher temperature levels, as the bearing factors in the

bearing resistance calculation were increased from temperature levels lower than 300 °C to larger than 600 °C, as shown in Yan and Young (2012). Therefore, for the same specimen series, the bearing strength as the minimum at the ambient temperature condition could not be the case at high temperature conditions. Figs. 7-8 illustrate the failure specimens for series 042-D and 190-D at ambient temperature condition. Figs. 9-12 show the failure specimens for series 042-D-d, 042-D-5d, 190-D-d and 190-D-5d at different high temperature conditions, respectively.

EFFECTS OF TEMPERATURE

Ultimate loads

Investigation on the influence of temperature (T) on the ultimate loads ($P_{u,r}$ and $P_{u,h}$) of double shear bolted connections were also conducted, where the e_1 in each specimen series was maintained. Generally, it was found that the ultimate loads ($P_{u,r}$ and $P_{u,h}$) decreased as the temperature increased for both specimen series 042-D and 190-D under the same values of e_1/d, as shown in Figs. 5-6. For the purpose of direct comparison, the strength reductions for each specimen series with the same e_1 at elevated temperatures was obtained by the factors of $P_{u,h}/P_{u,r}$. The factors of $P_{u,h}/P_{u,r}$ for the specimen series 042-D and 190-D are plotted in the vertical axes of Figs. 13-14, respectively; while the horizontal axes of the figures show the specimen temperatures. In each figure, the corresponding reduction factors of material properties ($f_{0.2,h}/f_{0.2,r}$ and $f_{u,h}/f_{u,r}$) at elevated temperatures are included. It was found that for

both specimen series, the reduction trends were similar at elevated temperatures, except for specimen Series 042-D-d, where larger reductions were found at the temperature levels of 300 °C and 450 °C. This may indicate that the effects of temperature on the strength reduction, i.e., $P_{u,h}/P_{u,r}$, are generally similar for each specimen series. The reduction trends of the ultimate load ($P_{u,h}$ and $P_{u,r}$) are generally similar to those of the corresponding $f_{0.2,h}/f_{0.2,r}$ and $f_{u,h}/f_{u,r}$ (see Figs. 13-14). The reduction factors of $f_{0.2,h}/f_{0.2,r}$ and $f_{u,h}/f_{u,r}$ generally provide conservative predictions of $P_{u,h}/P_{u,r}$ for all the specimen series, (i.e., series 042-D and 190-D) with different values of e_1, except for some specimens fabricated by TSS 0.42 mm tested at the temperature level of 300 °C. In addition, some specimens fabricated from TSS 1.90 mm G450 had relatively larger ultimate loads at the nominal temperature level of 300 °C compared with those tested at 22 °C (see Figs. 6 and 14), i.e., for specimen series 190-D-d, 190-D-3d and 190-D-5d. The maximum difference of which was 7.9%, namely, the ultimate load of 33.25 kN at 22 °C compared with that of 35.88 kN at 300 °C for Specimen 190-D-5d. This may be due to the ultimate stress at 300 °C is the same as that at 22 °C for TSS 1.90 mm G450 (see Tables 1 and 2). Furthermore, the higher bolted connection strengths could be due to the fact that the ultimate stress of cold-formed steel at 300 °C are higher than those at ambient temperature condition, as found by Kankanamge and Mahendran (2011), Imran et al. (2018), and Mahenthirarasa and Mahendran (2019). Imran et al. (2018) pointed out that this is due to the formation of Cottrell atmosphere, which leads to the serrations on the stress-strain curve (Portevin LeChatelier Effect) in the temperature range of 200 – 300 °C

Failure modes

As discussed earlier, Tables 4-8 reported the failures of the specimens tested at elevated temperatures. The specimen series 042-D-d, 042-D-3d, 190-D-d and 190-D-3d failed in tearout failure at elevated temperatures. This may indicate that the temperatures have little effect on

the failure mode of TSS bolted connections that failed in tearout. Bearing failure occurred in the specimen series 042-D-5d and 042-D-6d at temperature levels of 22 °C, 300 °C and 450 °C. However, the failure modes of both series changed to the material failure (MF) at the temperature levels of 600 °C and 900 °C (see Fig. 10(c)-(d)). Similarly, the bearing failure occurred in the specimen series 190-D-5d and 190-D-6d at the temperature levels of 22 °C, 300 °C, 450 °C and 600 °C. However, such failure mode of both series changed to the bolt shear failure at the temperature levels of 900 °C (see Fig. 12(d)). This may be because at higher temperature levels, larger bearing factors were obtained which led to higher bearing resistances of the specimens, as shown by Yan and Young (2012). In other words, the deteriorations of other connection strengths, e.g., bolt shear strength, could be worse than that of the bearing strength in the TSS bolted connections. Hence, for the same specimen series, the bearing strength as the minimum at the ambient temperature condition could not be the case at high temperature conditions, which lead to the change of the failure modes at elevated temperatures. It should be noted that bolt shear failure was deliberately avoided in the specimen designs at ambient temperature condition.

COMPARISON OF TEST RESULTS WITH PREDICTIONS

General

The predictions by the international design specifications (NAS 2016; EC3-1.3 2006; AS/NZS 2018) were assessed by comparing against the test results at elevated temperatures, including the ultimate loads and the corresponding failure modes. In the calculation of the predicted strengths, the previously discussed design rules were used. Note that these design rules are

applicable to ambient temperature condition only, but not to elevated temperatures. Hence, the material properties at ambient temperature were replaced directly by those at high temperatures in the calculation. Noted that for steel Grade 550, if the thickness is less than 0.6 mm, the reduced material properties of $f_{0.2}$ and f_u should be used as specified in Clause 1.5.1.1 of the AS/NZS (2018); while Section A3.1.3 in the NAS (2016) states that, for steels with elongation < 3%, the reduced material properties of $f_{0.2}$ and f_u should be used. These rules are only applicable to the TSS 0.42 mm G550 at the ambient temperature condition in this study. The effects of the reduced material properties on the predictions were investigated and discussed by Cai and Young (2019) for the bolted connections of TSS tested at ambient temperature condition. The investigation in the present paper is mainly focused on the bolted connections of TSS at elevated temperatures, hence, the reduced material properties were not considered in the strength calculations.

Comparison of test and predicted strengths

The minimum nominal strength was taken as the predicted strength of a bolted connection, where different failure modes were considered in the calculation except for the bolt shear failure mode. Note that bolt shear failure was deliberately avoided in the specimen design and this failure mode was not observed in the test results, except for specimens 190-D-5d and 190-D-6d at 900 °C. The specimens that failed in bolt shear were not included in the strength comparisons. Tables 4-8 show the comparisons between the ultimate loads ($P_{u,r}$ and $P_{u,r}$) from tests and the predicted strengths at different nominal temperature levels. Table 9 summarizes the comparisons of the ultimate loads from the tests with those from the predictions (NAS 2016; EC3-1.3 2006; AS/NZS 2018). In addition, the test results of $P_{u,r}/f_{u,r}dt$ and $P_{u,h}/f_{u,h}dt$ are plotted with the predicted curves from the different design specifications (NAS 2016; EC3-1.3 2006;

AS/NZS 2018) used in this study, as shown in Figs. 15-16, for specimen Series 042-D and 190-D, respectively.

It was found that the NAS (2016) and the EC3-1.3 (2006) predictions are generally conservative for the bolted connections at elevated temperatures in this study, where the EC3-1.3 (2006) provides more conservative but less scattered predictions, as shown in Tables 4-8. For example (See Table 4 at 22 °C), the mean values of $P_{u,r}/P_{NAS}$ and $P_{u,r}/P_{EC}$ are 1.23 and 1.51, respectively, with the corresponding coefficient of variation (COV) of 0.484 and 0.224. However, the AS/NZS (2018) predictions are generally unconservative for the connection specimens tested at ambient temperature (22 °C) and the nominal temperature level of 300 °C, for example, the mean value and COV of $P_{u,h}P_{AS/NZS}$ at 300 °C are 0.84 and 0.180, respectively. However, at the high temperature levels of 450 °C, 600 °C and 900 °C, the predictions by the AS/NZS (2018) become conservative, although less conservative and less scattered than those predicted by the NAS (2016) and the EC3-1.3 (2006) at the same temperature level (See Tables 6-8). For example (See Table 6 at 450 °C), the comparisons of $P_{u,r}/P_{AS/NZS}$, $P_{u,r}/P_{NAS}$ and $P_{u,r}/P_{EC}$ have the mean values of 1.13, 1.38 and 1.71, respectively, with the corresponding COV of 0.141, 0.288 and 0.193. Overall, the AS/NZS (2018) provides the least conservative and least scattered predictions for TSS double shear bolted connections at elevated temperatures, as summarized in Table 9.

Comparison of test and predicted failure modes

The predicted failure mode was determined by the failure associated with the predicted nominal strength for each specimen. Tables 4-8 show the corresponding predicted failure modes from the specifications (NAS 2016; EC3-1.3 2006; AS/NZS 2018) at different nominal temperature levels. As discussed previously, the effects of end distance (e_1) are incorporated by the coefficient of α_b in the calculation of strength failed by bearing in the EC3-1.3 (2006). Namely,

the failure modes between tearout failure (T) and bearing failure (B) are not distinguished by the EC3-1.3 (2006), where only bearing failure mode is predicted. However, the failure modes of tearout (shear fracture) and bearing are distinguished in predictions by the NAS (2016) and the AS/NZS (2018).

The accuracy of the predicted failure modes was assessed by comparing them with the failure modes from the tests, as shown in Tables 4-8. For the AS/NZS (2018) and the NAS (2016), the predictions are accurate for both specimen series (042-D and 190-D) at ambient temperature condition. Furthermore, the predicted failure modes are generally accurate for both specimen series at different high temperature levels. Material failure occurred in the specimens 042-D-5d and 042-D-6d at 600 °C and 900 °C, while bearing failure mode was predicted by AS/NZS (2018) and NAS (2016). The specimens 190-D-5d and 190-D-6d failed in bolt shear at 900 °C, which was not predicted by the specifications. As explained previously, bolt shear strengths were not considered in the predictions as this study focused mainly on the failure of connection plates. Hence, failure of bolts was deliberately avoided in the design of specimens at ambient temperature condition. Generally, the NAS (2016) and the AS/NZS (2018) could accurately predict the specimens that failed in tearout and bearing at different temperature levels. However, for the EC3-1.3 (2006), only the failure mode of plate bearing was predicted for all the connection specimens at different temperature levels.

CONCLUSIONS

In this study, the effects of end distance (e_1) and temperature on thin sheet steel (TSS) double shear bolted connections were experimentally investigated. A total of 43 connection specimens

were designed. The connection specimens were fabricated by TSS 0.42 mm G550 and 1.90 mm G450. The specimens were designed with the variation of e_1, and were categorized into two series by the ratio of the bolt diameter to thickness of the connection plate. In each series, the e_1 of the connection specimen was varied as 1.0d, 3d, 5d and 6d. The specimens were tested by the steady state test method at 5 different nominal temperature levels, namely, at 22 °C (ambient temperature), 300 °C, 450 °C, 600 °C and 900 °C. The material properties of the TSS 0.42 mm G550 and 1.90 mm G450 at elevated temperatures were measured. The structural behavior of the connections was investigated in terms of load-deflection curves, ultimate loads and failure modes.

The ultimate loads of the specimens are increased obviously with the increment of e_1/d from 1 to 5 at different nominal temperature levels. At each temperature level, the increments of ultimate loads are larger from $e_1/d = 1$ to $e_1/d = 3$ than those from $e_1/d = 3$ to $e_1/d = 5$. Generally, the ultimate loads are maintained when e_1/d is increased from 5 to 6. For each connection specimen series with the same value of e_1/d, it is shown that the effects of temperature on ultimate load reduction are generally similar for all test series. The reduction trends of the ultimate loads ($P_{u,h}$ and $P_{u,r}$) are generally similar to those of the corresponding material properties of $f_{0.2,h}/f_{0.2,r}$ and $f_{u,h}/f_{u,r}$ at elevated temperatures. The reduction factors of $f_{0.2,h}/f_{0.2,r}$ and $f_{u,h}/f_{u,r}$ generally provide conservative predictions for those of $P_{u,h}/P_{u,r}$, except for that of specimen Series 042-D at the temperature level of 300 °C. The connection specimens all failed in tearout for $e_1 = d$ and $e_1 = 3d$ at elevated temperatures. At $e_1/d = 1$, the tearout failure mode of the specimens was obvious; while the tearout failure mode was less obvious when the end distance increased to $e_1 = 3d$. Generally, the failure mode of the specimens changed to plate bearing when $e_1 = 5d$ and $e_1 = 6d$ at elevated temperatures.

The predictions by the international cold-formed steel design specifications, i.e., the North American Specification (NAS 2016), European Code (EC3-1.3 2006) and the Australian/New Zealand Standard (AS/NZS 2018), were assessed by comparing against the test results at elevated temperatures, including the ultimate loads and the corresponding failure modes. In the calculation of the predicted strengths, the material properties at ambient temperature were replaced directly by those at elevated temperatures. Overall, it was found that the predictions from the NAS (2016), EC3-1.3 (2006) and AS/NZS (2018) are conservative for TSS double shear bolted connections at elevated temperatures. The AS/NZS (2018) provides the least conservative and least scattered predictions, while the EC3-1.3 (2006) provides less conservative but more scattered predictions than the NAS (2016). Generally, the NAS (2016) and AS/NZS (2018) can provide accurate predictions of failure modes for double shear bolted connections that failed by tearout and bearing at elevated temperatures, except for those failed in material failure or bolt shear failure. However, the EC3-1.3 (2006) provides only bearing failure prediction for all the specimens at elevated temperatures.

REFERENCES

AS/NZS (2018). "Cold-formed Steel Structures." Australian/New Zealand Standard, AS/NZS4600:2018, Sydney, Australia, Standards Australia.

Cai, Y., and Young, B. (2014). "Structural behavior of cold-formed stainless steel bolted connections." *Thin-Walled Structures*, 83: 147-156.

Cai, Y., and Young, B. (2015). “High temperature tests of cold-formed stainless steel double shear bolted connections.” *Journal of Constructional Steel Research*, 104, 49-63.

Cai, Y., and Young, B. (2019). “Effects of end distance on thin sheet steel bolted connections.” *Engineering Structures*, 196, 109331.

Craveiro, H. D., Rodrigues, J. C. and Laím L. (2014) “Cold-formed steel columns made with open cross-sections subjected to fire.” *Thin-Walled Structures*, 851–14.

Craveiro, H. D., Rodrigues, J. C. and Laím L. (2016) “Experimental analysis of built-up closed cold-formed steel columns with restrained thermal elongation under fire conditions.” *Thin-Walled Structures*, 107, 564–579.

EC3-1.3 (2006). “Eurocode3—Design of Steel Structures—Part 1–3: General Rules Supplementary Rules for Cold-formed Members and Sheeting.” Brussels: European Committee for Standardization, EN1993-1-3:2006.

Imran, M., Mahendran, M. and Keerthan, P. (2018). “Mechanical properties of cold-formed steel tubular sections at elevated temperatures”, *Journal of Constructional Steel Research*, 143, 131-147.

Kankanamge N. D. and Mahendran M. (2011). “Mechanical properties of cold-formed steels at elevated temperatures.” *Thin-Walled Structures*, 49 26-44.

Laím, L., Rodrigues, J.P.C., and da Silva, L.S. (2013). “Experimental and numerical analysis on the structural behaviour of cold-formed steel beams.” *Thin-Walled Structures*, 1–13.

Laím, L., Rodrigues, J. C. and Craveiro H. D. (2015) “Flexural behavior of beams made of cold-formed steel sigma-shaped sections at ambient and fire conditions.” *Thin-Walled Structures*, 87, 53–65.

Laím, L., Rodrigues, J. C. and Craveiro H. D. (2016) “Flexural behavior of axially and rotationally restrained cold-formed steel beams subjected to fire.” *Thin-Walled Structures*, 98, 39–47.

Mahenthirarasa R. and Mahendran M. “Elevated Temperature Mechanical Properties of Cold-rolled Steel Sheets and Cold-formed Steel sections.” 9th International Conference on Steel and Aluminium Structures (ICSAS19), Bradford, UK, 3-5, July, 2019.

NAS (2016). “North American Specification for the Design of Cold-Formed Steel Structural Members.” American Iron and Steel Institute, AISI S100-2016, AISI Standard.

Rogers, C.A., and Hancock, G.J. (1998). “Bolted connection tests of thin G550 and G300 sheet steels.” *Journal of Structural Engineering*, 124(7), 798–808.

Rogers, C.A., and Hancock, G.J. (1999). “Bolted connection design for sheet steels less than 1.0 mm thick.” *Journal of Constructional Steel Research*, 51, 123–146.

Teh, L.H., and Clements, D.D.A. (2012). “Block shear capacity of bolted connections in cold-reduced steel sheets.” *Journal of Structural Engineering*, 138(4): 459–67.

Teh, L.H., and Uz, M.E. (2014). “Effect of loading direction on the bearing capacity of cold-reduced steel sheets.” *Journal of Structural Engineering*,140, 06014005-1-5.

Torabian, S., Zheng, B., and Schafer, B.W. (2015). “Experimental response of cold-formed steel lipped channel beam-columns.” *Thin-Walled Structures*, 89, 152–168.

Torabian, S., Fratamico, D.C., and Schafer, B.W. (2016). “Experimental response of cold-formed steel Zee-section beam-columns.” *Thin-Walled Structures*, 98: 496-517.

Wang, L., and Young, B. (2014). “Design of cold-formed steel channels with stiffened webs subjected to bending.” *Thin Walled Structures*, 85, 81-92.

Wang, L., and Young, B. (2016a). “Behavior of Cold-Formed Steel Built-Up Sections with Intermediate Stiffeners under Bending. I: Tests and Numerical Validation.” *Journal of Structural Engineering*, 142(3), 04015150-1-9.

Wang, L., and Young, B. (2016b). “Behavior of Cold-Formed Steel Built-Up Sections with Intermediate Stiffeners under Bending. II: Parametric Study and Design.” *Journal of Structural Engineering*, 142(3), 04015151-1-11.

Yan S., and Young, B. (2011). “Tests of single shear bolted connections of thin sheet steels at elevated temperatures - Part I: steady state tests.” *Thin-Walled Structures,* 49,1320–33.

Yan, S., and Young, B. (2012). “Bearing factors for single shear bolted connections of thin sheet steels at elevated temperatures.” *Thin-Walled Structures,* 52, 126–142.

Yan, S., and Young, B. (2013). “Effects of Elevated Temperatures on Double Shear Bolted Connections of Thin Sheet Steels.” *Journal of Structural Engineering*, 139, 757-771.

Young, B., and Hancock, G.J. (2003). “Compression tests of channels with inclined simple edge stiffeners.” *Journal of Structural Engineering*, 129(10), 1403–1411.

Young, B., and Rasmussen, K.J.R. (1998) “Design of lipped channel columns.” *Journal of Structural Engineering*, 124(2), 140–148.

Table 1. Material properties of thin sheet steel (TSS) at ambient temperature

Steel grades	E_r (GPa)	$f_{0.2,r}$ (MPa)	$f_{u,r}$ (MPa)	$\varepsilon_{u,r}$ (%)	$\varepsilon_{f,r}$ (%)
G550	228	730	743	0.5	2.9
G450	213	512	543	7.2	15.9

Source: Data from Cai and Young (2019).

Table 2. Material properties of TSS at high temperatures

Steel grades	T_m (°C)	E_h (GPa)	$f_{0.2,h}$ (MPa)	$f_{u,h}$ (MPa)	$\varepsilon_{u,h}$ (%)	$\varepsilon_{f,h}$ (%)
G550	296.8	215	585	673	3.3	10.1
	457.9	125	290	371	2.2	10.1
	602.0	105	59	88	14.1	51.3
	898.6	6.5	24	46	5.2	11.8
G450	295.9	209	465	543	5.6	18.5
	457.3	120	266	297	2.1	26.0
	601.3	109	57	87	12.0	59.7
	902.8	42	25	34	4.8	20.3

Table 3. Design of bolted connection specimens in double shear

Steel grades	t (mm)	d (mm)	e_1	T (°C)
G550	0.42	8	d, 3d, 5d, and 6d	22*, 300, 450, 600 and 900
G450	1.90			

Note: * means at ambient (room) temperature condition.

Table 4. Test results and comparison of TSS bolted connections at 22 °C

Specimen labeling	$P_{u,r}$ (kN)	$P_{u,r}/P_{AS/NZS}$	$P_{u,r}/P_{NAS}$	$P_{u,r}/P_{EC}$	Failure mode			
					Test	AS/NZS	NAS	EC
042-D-d	3.88	1.39	2.65	2.22	T	T	T	B
042-D-3d	6.81	0.81	0.83	1.30	T	T	T	B
042-D-5d	7.68	0.90	0.90	1.47	B	B	B	B
042-D-6d	7.44	0.87	0.87	1.42	B	B	B	B
190-D-d	7.57	0.91	1.73	1.09	T	T	T	B
190-D-3d	24.25	0.97	0.99	1.16	T	T	T	B
190-D-5d	33.25	1.00	1.00	1.59	B	B	B	B
190-D-6d	34.64	1.04	1.04	1.66	B	B	B	B
190-D-6d-r	34.85	1.05	1.05	1.67	B	B	B	B
Mean		0.99	1.23	1.51				
COV		0.169	0.484	0.224				

Note: T = Tearout; B = Bearing.

Table 5. Test results and comparison of TSS bolted connections at nominal temperature of 300 °C

Specimen labeling	T_m (°C)	$P_{u,h}$ (kN)	$P_{u,h}/P_{AS/NZS}$	$P_{u,h}/P_{NAS}$	$P_{u,h}/P_{EC}$	Failure mode			
						Test	AS/NZS	NAS	EC
042-D-d	300.8	1.97	0.78	1.48	1.24	T	T	T	B
042-D-3d	298.6	5.32	0.70	0.72	1.12	T	T	T	B
042-D-3d-r	299.2	4.94	0.65	0.67	1.04	T	T	T	B
042-D-5d	299.3	5.07	0.66	0.66	1.07	B	B	B	B
042-D-6d	297.6	5.90	0.76	0.76	1.24	B	B	B	B
190-D-d	349.7	7.50	0.90	1.71	1.08	T	T	T	B
190-D-d-r	302.5	7.97	0.96	1.82	1.15	T	T	T	B
190-D-3d	312.6	25.15	1.01	1.03	1.21	T	T	T	B
190-D-5d	311.8	35.88	1.08	1.08	1.72	B	B	B	B
190-D-6d	319.4	30.46	0.92	0.92	1.46	B	B	B	B
Mean			0.84	1.08	1.23				
COV			0.180	0.403	0.171				

Table 6. Test results and comparison of TSS bolted connections at nominal temperature of 450 °C

Specimen labeling	T_m (°C)	$P_{u,h}$ (kN)	$P_{u,h}/P_{AS/NZS}$	$P_{u,h}/P_{NAS}$	$P_{u,h}/P_{EC}$	Failure mode			
						Test	AS/NZS	NAS	EC
042-D-d	448.2	1.47	1.05	2.01	1.69	T	T	T	B
042-D-3d	450.8	4.13	0.99	1.01	1.58	T	T	T	B
042-D-5d	451.5	4.35	1.02	1.02	1.66	B	B	B	B
042-D-6d	449.5	4.44	1.04	1.04	1.70	B	B	B	B
190-D-d	501.5	4.64	1.02	1.94	1.22	T	T	T	B
190-D-3d	449.8	16.73	1.22	1.25	1.47	T	T	T	B
190-D-5d	458.2	25.24	1.39	1.39	2.21	B	B	B	B
190-D-6d	460.5	24.48	1.34	1.34	2.15	B	B	B	B
Mean			1.13	1.38	1.71				
COV			0.141	0.288	0.193				

Table 7. Test results and comparison of TSS bolted connections at nominal temperature of 600 °C

Specimen labeling	T_m (°C)	$P_{u,h}$ (kN)	$P_{u,h}/P_{AS/NZS}$	$P_{u,h}/P_{NAS}$	$P_{u,h}/P_{EC}$	Failure mode			
						Test	AS/NZS	NAS	EC
042-D-d	604.9	0.87	2.63	5.01	4.20	T	T	T	B
042-D-3d	600.8	1.67	1.68	1.73	2.69	T	T	T	B
042-D-5d	605.2	1.68	1.66	1.66	2.71	MF	B	B	B
042-D-6d	609.3	1.40	1.38	1.38	2.26	MF	B	B	B
190-D-d	608.8	2.06	1.54	2.94	1.85	T	T	T	B
190-D-3d	610.8	5.09	1.27	1.30	1.52	T	T	T	B
190-D-5d	611.5	7.20	1.35	1.35	2.16	B	B	B	B
190-D-6d	614.2	6.92	1.30	1.30	2.07	B	B	B	B
Mean			1.60	2.08	2.43				
COV			0.277	0.624	0.336				

Note: MF = Material failure.

Table 8. Test results and comparison of TSS bolted connections at nominal temperature of 900 °C

Specimen labeling	T_m (°C)	$P_{u,h}$ (kN)	$P_{u,h}/P_{AS/NZS}$	$P_{u,h}/P_{NAS}$	$P_{u,h}/P_{EC}$	Failure mode			
						Test	AS/NZS	NAS	EC
042-D-d	900.6	0.37	2.14	4.07	3.42	T	T	T	B
042-D-3d	899.6	0.59	1.14	1.17	1.82	T	T	T	B
042-D-5d	901.1	0.59	1.12	1.12	1.82	MF	B	B	B
042-D-6d	900.8	0.61	1.15	1.15	1.88	MF	B	B	B
190-D-d	898.8	0.81	1.55	2.95	1.86	T	T	T	B
190-D-3d	904.6	1.98	1.26	1.30	1.52	T	T	T	B
190-D-5d	905.9	2.26	-	-	-	BS	-	-	-
190-D-6d	901.3	2.21	-	-	-	BS	-	-	-
Mean			1.39	1.96	2.05				
COV			0.287	0.641	0.333				

Note: BS = Bolt shear.

Table 9. Summary of comparison for TSS double shear bolted connections at elevated temperatures

Specimen series	Total number		$P_{u,r}/P_{AS/NZS}$ and $P_{u,h}/P_{AS/NZS}$	$P_{u,r}/P_{NAS}$ and $P_{u,h}/P_{NAS}$	$P_{u,r}/P_{EC}$ and $P_{u,h}/P_{EC}$
042-D and 190-D	43	Mean	1.16	1.50	1.74
		COV	0.333	0.597	0.370

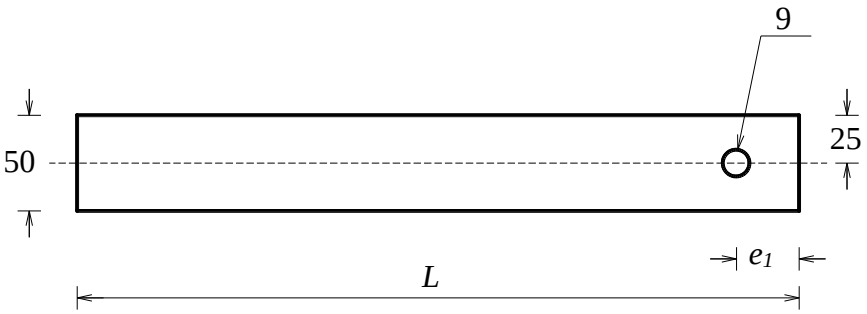

Fig. 1. Definition of symbols

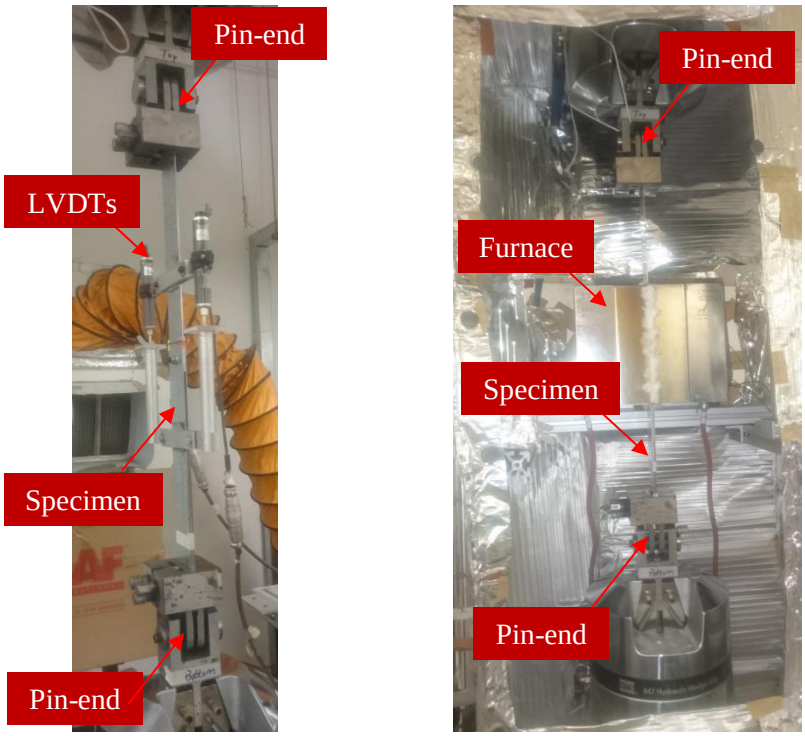

Fig. 2. Test setup of TSS double shear bolted connecitons at ambient (*left*) and high temperatures (*right*)

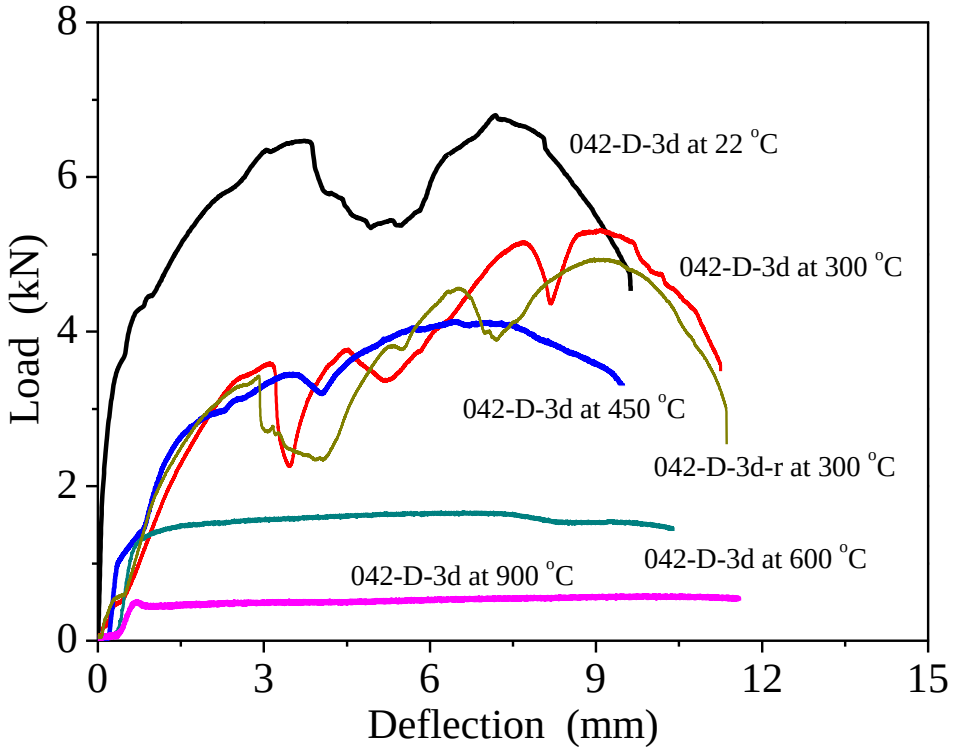

Fig. 3. Load-deflection curves of specimen Series 042-D-3d at elevated temperatures

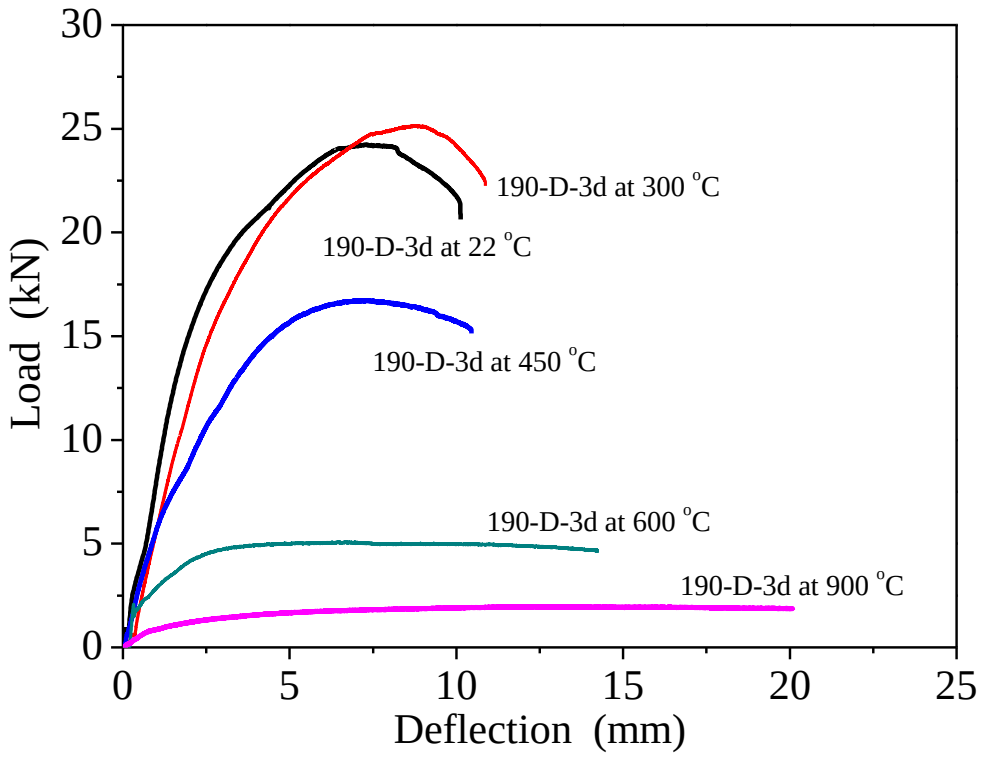

Fig. 4. Load-deflection curves of specimen Series 190-D-3d at elevated temperatures

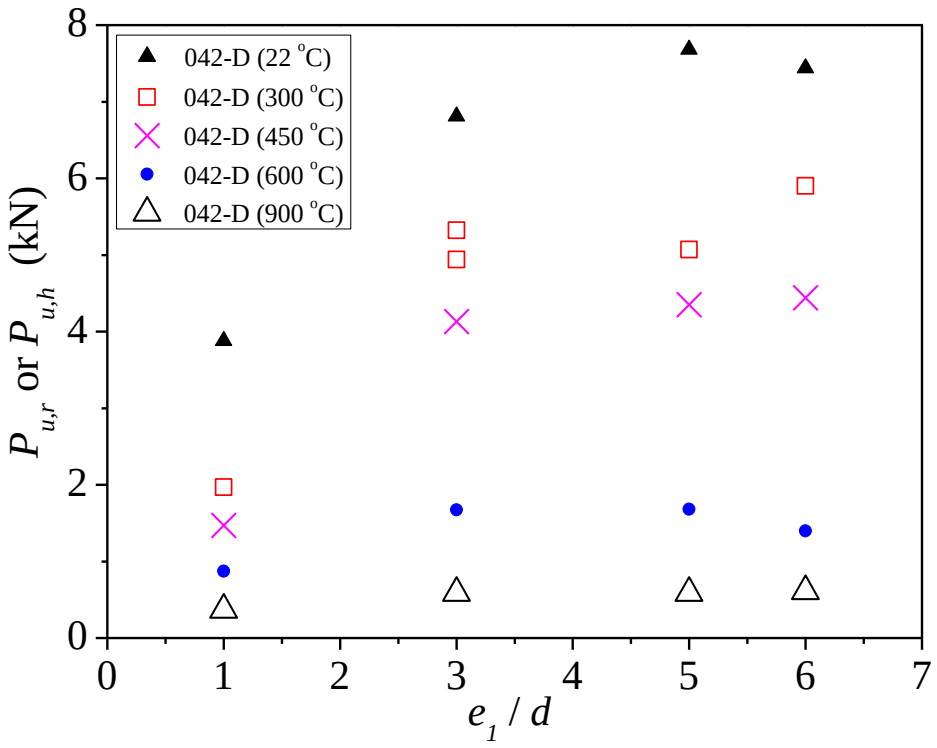

Fig. 5. Effects of e_1 on connection specimens Series 042-D at elevated temperatures

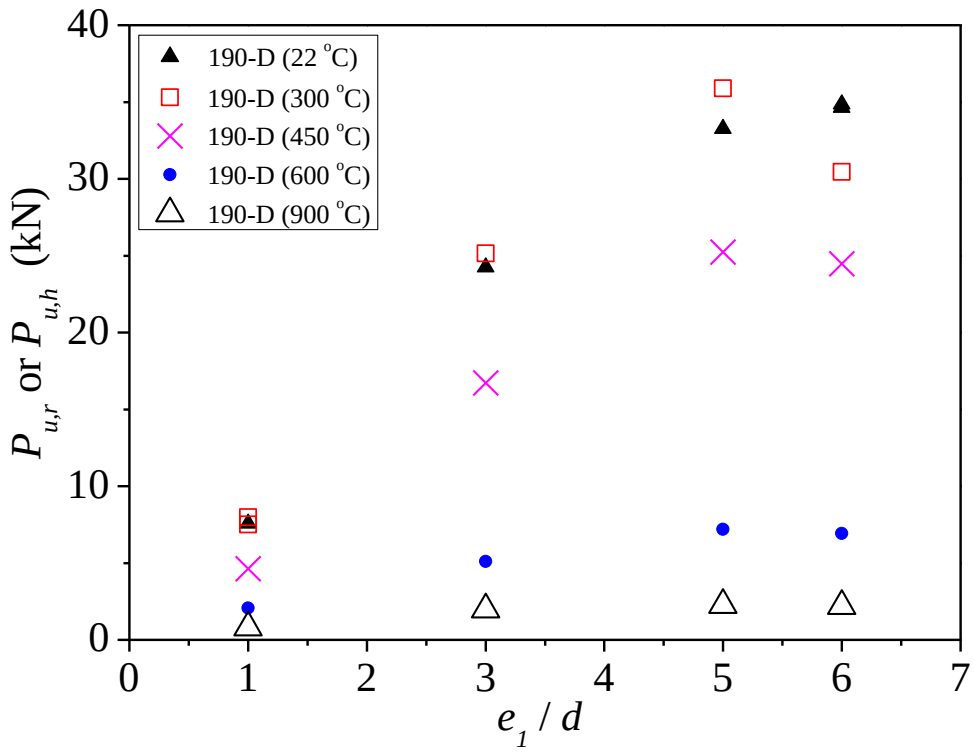

Fig. 6. Effects of e_1 on connection specimens Series 190-D at elevated temperatures

Fig. 7. Effects of e_1 on failure modes of specimen Series 042-D at ambient temperature
(a) 042-D-d

Fig. 7. Effects of e_1 on failure modes of specimen Series 042-D at ambient temperature
(b) 042-D-3d

Fig. 7. Effects of e_1 on failure modes of specimen Series 042-D at ambient temperature
(c) 042-D-5d

Fig. 7. Effects of e_1 on failure modes of specimen Series 042-D at ambient temperature
(d) 042-D-6d

Fig. 8. Effects of e_1 on failure modes of specimen Series 190-D at ambient temperature (a) 190-D-d

Fig. 8. Effects of e_1 on failure modes of specimen Series 190-D at ambient temperature (b) 190-D-3d

Fig. 8. Effects of e_1 on failure modes of specimen Series 190-D at ambient temperature
(c) 190-D-5d

Fig. 8. Effects of e_1 on failure modes of specimen Series 190-D at ambient temperature
(d) 190-D-6d

Fig. 9. Effects of *T* on failure modes of specimen Series 042-D-d
(a) 300 °C

Fig. 9. Effects of *T* on failure modes of specimen Series 042-D-d
(b) 450 °C

Fig. 9. Effects of *T* on failure modes of specimen Series 042-D-d
(c) 600 °C

Fig. 9. Effects of *T* on failure modes of specimen Series 042-D-d
(d) 900 °C

Fig. 10. Effects of *T* on failure modes of specimen Series 042-D-5d
(a) 300 °C

Fig. 10. Effects of *T* on failure modes of specimen Series 042-D-5d
(b) 450 °C

Fig. 10. Effects of *T* on failure modes of specimen Series 042-D-5d
(c) 600 °C

Fig. 10. Effects of *T* on failure modes of specimen Series 042-D-5d
(d) 900 °C

Fig. 11. Effects of *T* on failure modes of specimen Series 190-D-d
(a) 300 °C

Fig. 11. Effects of *T* on failure modes of specimen Series 190-D-d
(b) 450 °C

Fig. 11. Effects of *T* on failure modes of specimen Series 190-D-d
(c) 600 °C

Fig. 11. Effects of *T* on failure modes of specimen Series 190-D-d
(d) 900 °C

Fig. 12. Effects of *T* on failure modes of specimen Series 190-D-5d
(a) 300 °C

Fig. 12. Effects of *T* on failure modes of specimen Series 190-D-5d
(b) 450 °C

Fig. 12. Effects of *T* on failure modes of specimen Series 190-D-5d
(c) 600 °C

Fig. 12. Effects of *T* on failure modes of specimen Series 190-D-5d
(d) 900 °C

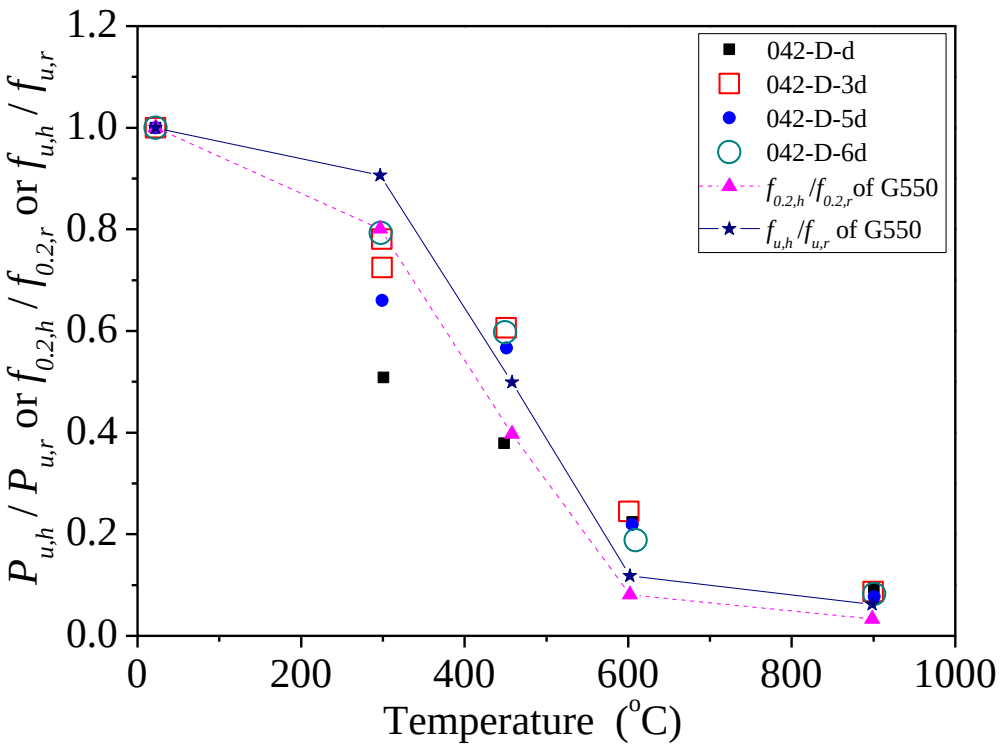

Fig. 13. Effects of *T* on connection specimens Series 042-D

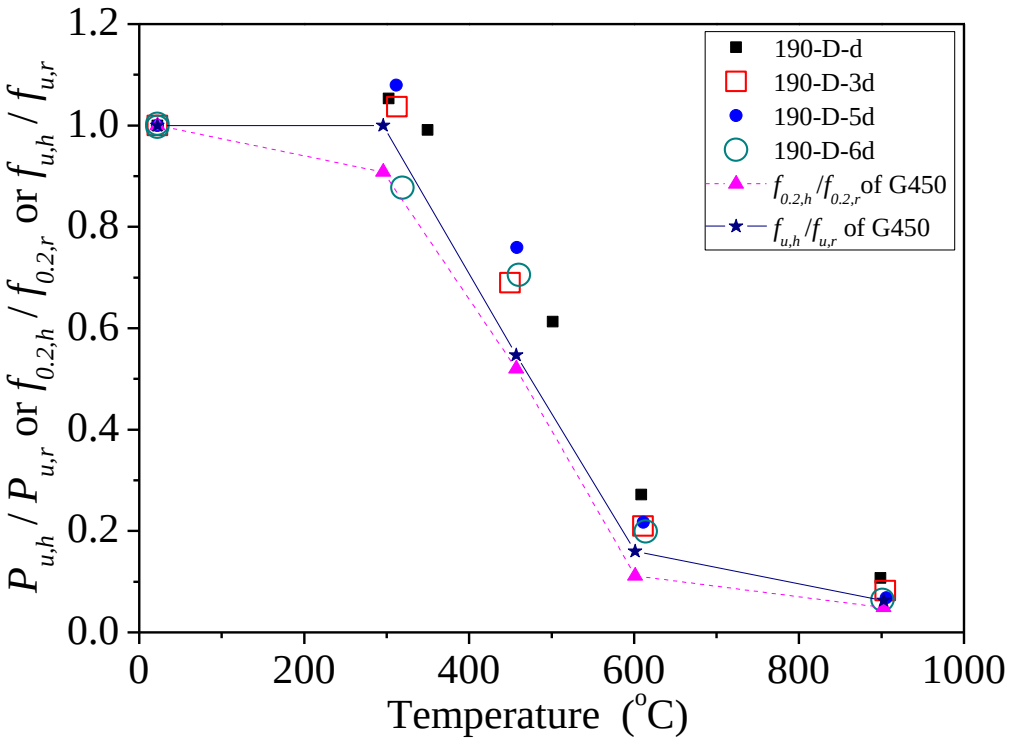

Fig. 14. Effects of *T* on connection specimens Series 190-D

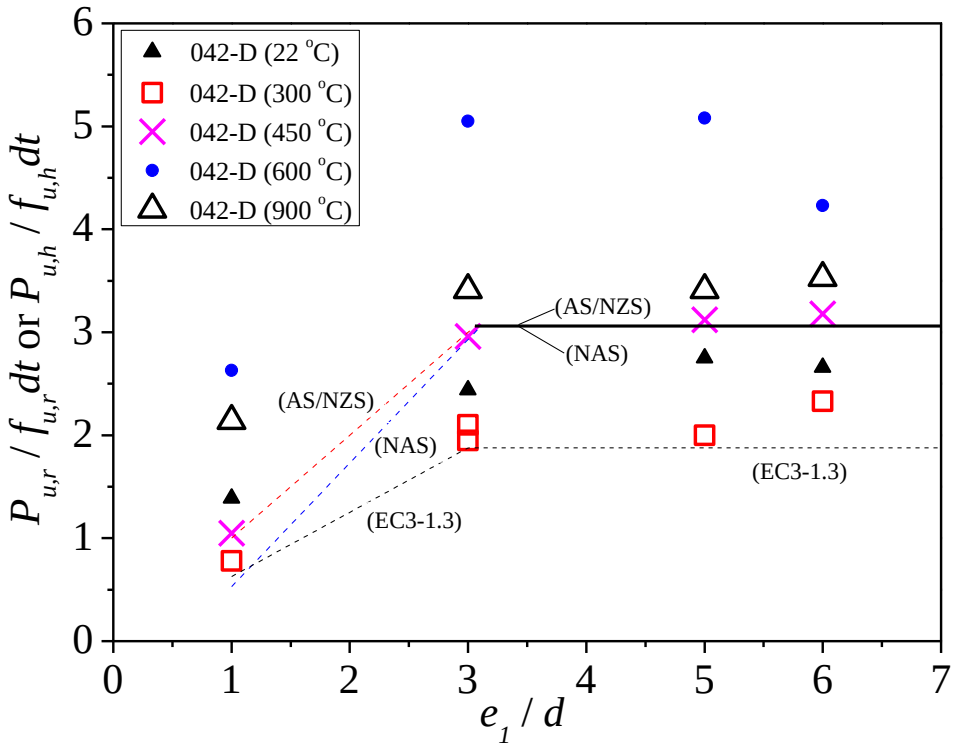

Fig. 15. Comparison of test results with predicted strengths for specimen Series 042-D

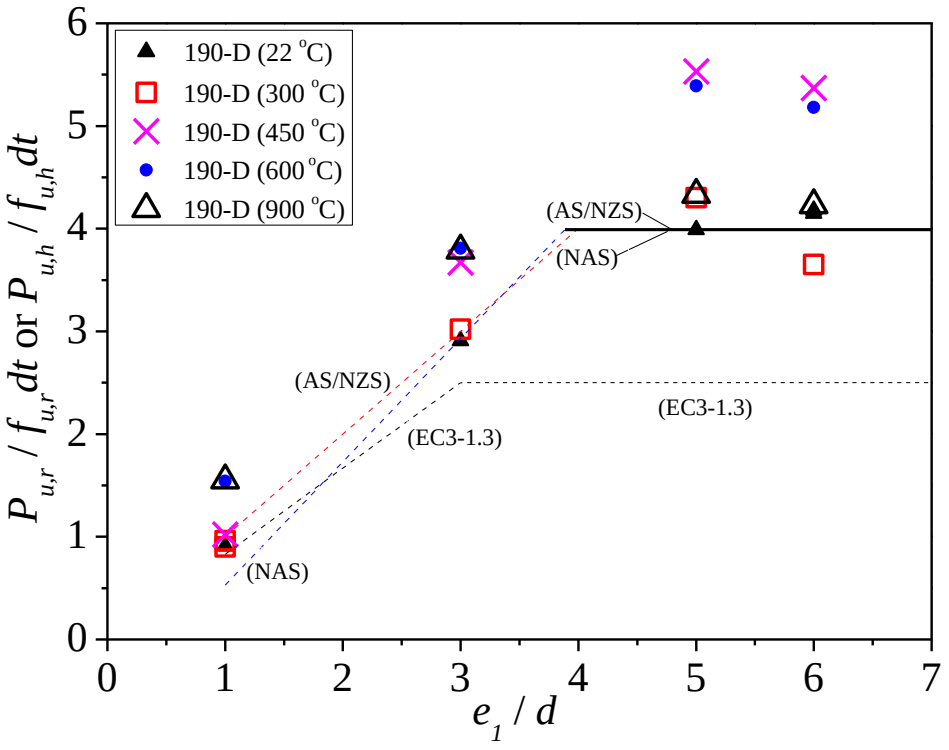

Fig. 16. Comparison of test results with predicted strengths for specimen Series 190-D